Journal of Steroid Biochemistry & Molecular Biology 122 (2010) 53–64

Contents lists available at ScienceDirect

Journal of Steroid Biochemistry and Molecular Biology

journal homepage: www.elsevier.com/locate/jsbmb

A single dose of dihydrotestosterone induced a myogenic transcriptional program in female intra-abdominal adipose tissue

Maria Rita De Giorgio[a,b], Mayumi Yoshioka[a,b], Jonny St-Amand[a,b,*]

[a] Functional Genomics Laboratory, Molecular Endocrinology and Oncology Research Center, Laval University Medical Center, Québec City, Canada
[b] Department of Anatomy and Physiology, Laval University, Québec City, Canada

ARTICLE INFO

Article history:
Received 31 July 2009
Received in revised form 14 February 2010
Accepted 24 February 2010

Keywords:
Retroperitoneal fat tissue
Androgens
SAGE
Myogenic-like transcriptome

ABSTRACT

Sex steroids are key regulators of adipose tissue (AT) mass, determining gender-specific differences in fat distribution and accumulation. With the aim of exploring the relevance and peculiarities of androgen action in female intra-abdominal AT, we used the serial analysis of gene expression (SAGE) method to analyze the AT transcriptome in four groups of female mice: intact, ovariectomized (OVX), OVX plus dihydrotestosterone (DHT) injection at 3 h or 24 h before sacrifice (DHT3 h, DHT24 h). An average of 19 555 transcript species was examined in retroperitoneal fat. We found a total of 321 transcripts differentially modulated by DHT and OVX, including 125 novel genes. Several genes involved in energy metabolism/ATP production were up-regulated by DHT, whereas important regulators of lipid metabolism were reduced. Transcripts involved in Ca^{2+} uptake/release, cell signalling, cell defence and protein expression were differentially modulated by DHT. A surprising number of myogenic genes were up-regulated, including myosin light and heavy polypeptides, troponins, as well as several actin-binding proteins. These results suggest that DHT24 h may have induced a myogenic-like transcriptional program in adipocytes. The present study sheds light on the distinctive female transcriptional pattern acutely induced by androgens in intra-abdominal fat, and may add new insights into the global understanding of menopausal endocrinology and its association to intra-abdominal obesity.

1. Introduction

During menopause, and particularly during the transition period also called interphase [1,2], women's hormone profile undergoes crucial changes which may profoundly affect their life and health conditions. The key event is the shift of sex hormone balance, which essentially alters the relative proportions of estrogen and androgen secretion, and their circulating levels. Specifically, in the early menopausal phases, the progressive decline of estrogen levels is accompanied by a more gradual fall of androgen ones, leading to a prolonged condition of androgenicity [1,2]. This has an important impact on adipose tissue (AT) regulation and distribution, with an increase in total and central adiposity, and a simultaneous loss in fat-free mass [3]. Moreover, androgen excess has been associated to an increased risk of type 2 diabetes/metabolic syndrome, obesity [4,5] and cardiovascular diseases (CVD), and a correlation has been suggested with the duration of exposure [1,6]. If we consider that CVD still represent the leading cause of death among postmenopausal women [7], the study of fine endocrine changes occurring in this phase appears of primary importance, and should be oriented to clarify the specific role of androgen-regulated pathways and their potential as therapeutic targets.

We have already analyzed the short- and long-term effects of dihydrotestosterone (DHT) in male mice AT, finding that various essential pathways were modulated [8,9]. In summary, our data from male AT have shown that DHT acutely stimulates glycolysis, fatty acids (FA) and triacylglycerol (TG) production, lypolisis and cell shape reorganization, influencing cell proliferation and differentiation [8]. The acute differential effects exerted by ovariectomy (OVX) and estradiol (E_2) on female mice AT have also been studied, showing a limited number of regulated transcripts [10].

The current study intended to identify the androgen-mediated molecular mechanisms which play a specific role in the regulation of female fat tissue. In particular, we were interested in identifying the transcriptional changes acutely induced by androgen in female intra-abdominal fat. In this attempt, we used the serial analysis of gene expression (SAGE) method and analyzed the retroperitoneal AT transcriptome of OVX mice, at 3 and 24 h after DHT administration (DHT3 h, DHT24 h). We found that major changes on gene expression occurred 24 h following DHT treatment. Surprisingly, lipid metabolism has been poorly affected by androgen treatment,

* Corresponding author at: Functional Genomics Laboratory, Molecular Endocrinology and Oncology Research Center, Laval University Medical Center (CHUL), 2705 Boul. Laurier, Québec (PQ) G1V 4G2, Canada. Tel.: +1 418 654 2296; fax: +1 418 654 2761.
E-mail address: Jonny.St-Amand@crchul.ulaval.ca (J. St-Amand).

0960-0760/$ – see front matter © 2010 Elsevier Ltd. All rights reserved.
doi:10.1016/j.jsbmb.2010.02.023

whereas an unexpected myogenic-like transcriptional program has been induced.

2. Materials and methods

2.1. Sample preparation

For these experiments, the retroperitoneal fat depot was chosen, as component of the intra-abdominal AT [11]. The tissue was obtained from C57BL6 female mice (14 per group), 14–15 weeks of age, purchased from Charles River Canada (St-Constant, Québec, Canada). The experiments were conducted in accordance with the requirements of the Canadian Council on Animal Care, and approved by the animal protection Committee of Laval University.

Animals were provided Laboratory Rodent Diet No. 5002 (PMI, St. Louis, MO) and water *ad libitum*. Intact mice were sham-operated. The other mice were ovariectomized 7 days before death (OVX), in order to have a reliable model of early menopause [12]. Vehicle (0.4%, w/v, Methocel A15LV Premium/5% ethanol) for the intact and OVX groups was injected 24 h before death. In the two treated groups, DHT (0.1 mg) was injected 3 h (DHT3 h) and 24 h (DHT24 h) prior to sacrifice. Time points were decided on the basis of previous transcriptomic studies [13,14], in which 3 h and 24 h time points had shown the highest transcriptional activity. The dose of DHT chosen, 0.1 mg, is the minimum dose needed to restore prostate size following castration in males [15], and has been previously administered as a physiological dose in other studies on both male and female mice [14,16,17]. However, further specifications are needed in the case of female mice, in which the DHT dose considered may result in supraphysiological circulating levels, at least in the first 6 hours after the injection. In fact, as shown by Zhang et al. [18], at 3 h, DHT serum concentration should reach 5–6 ng/ml, and then gradually decrease to more physiological levels [19,20], being finally lower than 500 pg/ml (18–24 h). Immediately following the sacrifice, the retroperitoneal fat was dissected (between 09:00 and 12:15 h). The samples from all mice of the same group were pooled to eliminate inter-individual variations and to extract sufficient amount of mRNA. The tissues were frozen in liquid nitrogen, and stored at −80 °C until analysis.

2.2. Transcriptomic analysis

The four SAGE libraries were constructed as previously described [21,22]. Total RNA was isolated from pooled AT for each group ($n = 14$) by Trizol (Invitrogen Canada Inc., Burlington, ON). The quality of total RNA was monitored by micro-capillary electrophoresis (Bioanalizer 2100, Agilent Technologies, Mississauga, ON). Polyadenylated RNA was extracted with the Oligotex mRNA Mini Kit (Qiagen Inc., Mississauga, ON), annealed with the biotin-5′-T_{18}-3′ primer and converted to cDNA using the cDNA synthesis kit (Invitrogen Canada Inc.). The resulting cDNAs were digested with NlaIII (New England BioLabs Ltd., Pickering, ON), and the 3′ restriction fragments were captured using streptavidin-coated magnetic beads (Dynal Biotech LLC, Brown Deer, WI) and separated into two populations. Each population was ligated to one of two annealed linkers and extensively washed to remove unligated linkers [22]. The tag beside the most 3′ NlaIII restriction site (CATG) of each transcript was digested with BsmFI (New England BioLabs Ltd.), thereby releasing cDNA fragments including the short 15-bp tags. The blunting kit from Takara Bio Inc. (Otsu, Japan) was used for the blunting and ligation of the two tag populations. The resulting ligation products containing the ditags were amplified by PCR and digested with NlaIII. The band containing the ditags was extracted from the 12% polyacrylamide gel with Spin-X microcentrifuge tube (Fisher, Pittsburgh, PA) and the purified ditags were self-ligated to form concatemers using T4 ligase (Invitrogen Canada Inc.). The concatemers ranging from 500 bp to 1800 bp were isolated by agarose gel and extracted with Gene-Clean Spin (Qbiogene, Montreal, QC). The resulting DNA fragments were ligated into the SphI site of pUC19 and cloned into OmniMAX 2T1 competent cells (Invitrogen Canada Inc.). White colonies were picked up, and concatemer inserts were sequenced by the Applied Biosystems 3730 (Foster City, CA).

2.3. Bioinformatic analysis

Sequence files were analyzed using the SAGEana program, a modification of SAGEparser [23]. In brief, SAGE tags corresponding to linker sequences were discarded and replicate concatemers were counted only once. Identification of the transcripts was obtained by matching the 15 bp (sequence at the last CATG + 11 bp tags) with SAGEmap, UniGene and GenBank databases. Classification of the transcripts was based upon the updated information of the genome directory [24] found at the TIGR web site (http://www.tigr.org/), the SOURCE (http://genome-www5.stanford.edu/cgi-bin/source/sourceSearch) and the OMIM (http://www.ncbi.nlm.nih.gov/), as well as upon previously published literature. We have previously shown that the SAGE method is very reproducible with $r^2 = 0.96$ between two SAGE libraries generated from two cDNA libraries constructed from the same total RNA pool [23].

2.4. Validation by quantitative real-time PCR (Q_RT-PCR)

First strand cDNA was synthesized using 5 μg of pooled RNA of each experimental group in a reaction containing 200 U of Superscript III Rnase H-RT (Invitrogen Canada Inc.), 300 ng of oligo-dT_{18}, 500 μM deoxynucleotides triphosphate, 10 mM dithiothreitol and 34 U of human RNase inhibitor (Amersham Pharmacia, Piscataway, NJ) in a final volume of 50 μl. The resulting products were then treated with 1 μg of Rnase A for 30 min at 37 °C and purified thereafter with Qiaquick PCR purification kits (Qiagen). The cDNA corresponding to 20 ng of total RNA was used to perform fluorescent-based real-time PCR quantification using the LightCycler real-time PCR apparatus (Roche Inc., Nutley, NJ) and the FastStart DNA Master SYBR green kit (Roche Diagnostics). Reading of the fluorescence signal was taken at the end of the heating to avoid non-specific signal. A melting curve was performed to assess non-specific signals. Annealing temperature was selected based on contamination levels and melting curve results. Prior to mRNA quantification, RNA samples were also verified for genomic DNA contamination. Oligoprimer pairs that allow the amplification of approximately 250 bp were designed by GeneTools software (Biotools Inc., Edmonton, AB) and their specificity was verified by blast in GenBank database. Gene name, GenBank accession numbers and regions used for the primer pairs were the following: ATPase, Ca^{2+} transporting, cardiac muscle, fast twitch 1 (*Atp2a1*), NM_007504, 82–366; metallothionein 2 (*Mt2*), NM_016673, 1435–1724; myosin heavy polypeptide 1 (*Myh1*), AJ293626, 1108–1356; myosin heavy polypeptide 4 (*Myh4*), XM_126119, 1571–1693; troponin C, fast skeletal (*Tnnc2*), AV083137, 41–227; troponin T3, fast skeletal (*Tnnt3*), L48989, 417–544; tropomyosin 2, beta (*Tpm2*), M81086, 1720–1944. The mRNA levels were calculated using a standard curve of crossing point (Cp) versus logarithm of the quantity, and expressed as the number of copies per microgram of total RNA [25]. The LightCycler 3.5 program provided by the manufacturer (Roche Inc.) was used to calculate the Cp according to the second derivative and double correction method previously described by Luu-The et al. [25]. The standard curve with efficiency coefficient $E = 2$ was established

Table 1
Female mouse DHT-modulated transcripts involved in lipid metabolism.

Tag	Intact	OVX	OVX + DHT		Description (UniGene cluster, GenBank accession no.)
			3 h	24 h	
Fatty acid synthesis/lipogenesis					
CTATGTATCCG	31	31	**3** ↓	**6** ↓	EST carbonic anhydrase 3 (Mm.300, CB947072)
ATGCAGGGCCA	277	**114** ↓	255	121	Fatty acid synthase (Mm.236443; AF127033)
TTGTCAGGTAG	113	47	**142** ↑	86	Malic enzyme 1, NADP(+)-dependent, cytosolic, supernatant (Mm.148155; NM_008615)
GGCAAGTGCTA	83	32	7	**2** ↓	Stearoyl-coenzyme A desaturase 1 (Mm.267377, AF509570)
Beta-oxidation/lipolysis					
TGGGTGTCCAG	90	68	25	**6** ↓	Acyl-CoA synthetase long-chain family member 1 (Mm.210323; NM_007981)
CTGTGGAATGA	69	38	29	**9** ↓	Desnutrin (patatin-like phospholipase domain containing 2) (Mm.29998; AY731699)
ACAAGTCTCTG	91	79	31	**13** ↓	EST lipoprotein lipase (Mm.1514, AA537700)
TTTCTCCTGCC	16	16	7	**2** ↓	EST lipoprotein lipase (Mm.1514, BY490220)
Transport/regulation					
GGGTACAAGAC	32	24	8	**3** ↓	Adiponectin receptor 2 (Mm.291826, BC064109)
AATTATTTTGT	3	2	15	**16** ↑	Caveolin 2 (Mm.396075, AB049604)
CTGCATAGCTC	21	21	**73** ↑	**78** ↑	CD36 antigen (Mm.18628, AK052825)
GTTTTCCCCTC	2	1	3	**44** ↑	Fatty acid binding protein 3, muscle and heart (Mm.22220, NM_010174)
AGCCAAAGGAA	718	570	**1371** ↑	**7**71	Fatty acid binding protein 4, adipocyte (Mm.582, AK088535)
ATCATCAGCGT	63	43	**3** ↓	**3** ↓	EST fatty acid binding protein 4, adipocyte (Mm.582, BG794981)
CAGAGCTGCTT	1	1	3	**16** ↑	EST protein kinase, AMP-activated, beta 2 non-catalytic subunit (Mm.31175, BG794097)
CCACTGTGTCC	51	36	25	**6** ↓	Resistin (Mm.1181, AF290870)
CAAAAATAGTA	10	5	**29** ↑	**17**	Sulfotransferase family 1A, phenol-preferring, member 1 (Mm.368982; BC005413)

Abbreviations: OVX, ovariectomy; DHT, dihydrotestosterone. Numbers indicate the count of serial analysis of gene expression (SAGE) tags per 100 000. SAGE tag numbers in bold indicate a statistical significance ($P \leq 0.05$; OVX vs. intact, DHT vs. OVX).

using known cDNA amounts of 0, 10^2, 10^3, 10^4, 10^5 and 10^6 copies of ATP synthase O subunit.

2.5. Statistical analysis

The significant difference was set at $P \leq 0.05$. For the SAGE data, the comparative count display (CCD) test was used to identify the transcripts which were significantly differentially expressed ($P < 0.02$, after Bonferroni adjustment) between the groups with more than a two-fold change. As previously described by Lash et al. [26], the CCD test makes a key-by-key comparison of two key-count distributions by generating a probability that the frequency of any key in the distribution differs by more than a given fold factor from the other distribution. The data were normalized to 100 000 tags for presentation.

3. Results

The SAGE libraries revealed an average of 44 181 SAGE tags per group, corresponding to 19 555 transcript species. Among these, only 14 transcripts were found to be differentially modulated by OVX, whereas 307 transcripts were regulated by DHT. In particular, 224 genes were up-regulated and 83 were down-regulated following DHT treatment. In total, 125 novel transcripts were significantly modulated.

3.1. DHT-modulated transcripts involved in lipid metabolism

Our data showed a general down-regulation of lipid metabolism-related transcripts following DHT24 h treatment, including both anabolic and catabolic genes (Table 1). However, at DHT3 h, only a few transcripts were modulated, including the up-regulation of malic enzyme 1 as well as fatty acid binding protein (*Fabp*) 4 and *Cd36*. At DHT24 h we observed a reduced expression of biosynthetic genes such as stearoyl-CoA desaturase 1, as well as a decreased transcription of genes involved in beta-oxidation/lipogenesis processes, such as acyl-CoA synthetase, desnutrin, expression sequenced tag (EST) *Lpl*. When we considered the regulatory transcripts which affect adipocyte metabolism, we found a diminished level of resistin and adiponectin receptor 2 gene expression, and an increase in caveolin 2, *Cd36* and EST *Ampkβ* subunit levels. Interestingly, we found the DHT24 h up-regulation of *Fabp3*, a transcript generally known to be expressed in muscle tissues.

3.2. DHT-modulated transcripts involved in glucose metabolism and energy production

DHT treatment positively influenced glucose metabolism, tricarboxylic acid cycle (TCA) and ATP synthesis processes, and these effects are prominent at DHT24 h when 59 transcripts were found to be differentially modulated compared to OVX control (Table 2). Numerous of these transcripts were mitochondrial, confirming that mitochondrial RNAs are polyadenylated [27]. Glycogen metabolism (protein phosphatase 1, glycogen phosphorylase and phosphoglucomutase 2) and glycolysis (phosphofructokinase, aldolase 1A, EST glyceraldehyde-3-phosphate dehydrogenase, and phosphoglycerate mutase 2) transcripts were up-regulated. Lactate dehydrogenase 2β chain gene expression was increased, as well as the transcription of many genes involved in TCA cycle reactions, such as aconitase 2, succinate-CoA ligase, and malate dehydrogenase 2. Overall, complex I (NADH dehydrogenase subunits 1α, 1β, 2, 3, 4), complex II (succinate dehydrogenase complex, subunit B), complex III (ubiquinol-cytochrome c reductase) and complex IV (cytochrome c oxidase subunit 1, 2, 3, 4a, 7a) of the mitochondrial electron transport chain were up-regulated. Consistently, the

Table 2
Female mouse DHT-modulated transcripts involved in glucose metabolism and energy production.

Tag	Intact	OVX	OVX + DHT		Description (UniGene cluster, GenBank accession number)
			3 h	24 h	
Glucose/aminoacid metabolism					
CCTACTAACCA	117	68	83	**594** ↑	Aldolase 1, A isoform (Mm.275831, NM_007438)
AGGTCCACCAC	4	2	3	**34** ↑	EST glyceraldehyde-3-phosphate dehydrogenase (Mm.339669, AV019029)
ACCGGTTTAAA	5	5	3	**46** ↑	Muscle glycogen phosphorylase (Mm.27806, AF124787)
TTGCTTTGTTG	88	39	**125** ↑	31	Phosphoenolpyruvate carboxykinase 1 (Mm.266867, NM_011044)
CCTGCAACCAG	3	5	4	**69** ↑	Phosphofructokinase, muscle (Mm.272582, BC005526)
TAATCCAACAG	18	13	16	**71** ↑	Phosphoglucomutase 2 (Mm.217764; NM_028132)
GAAGCTGTTGC	5	7	5	**321** ↑	Phosphoglycerate mutase 2 (Mm.219627, BC010750)
CTGGAAAAACA	1	3	3	**20** ↑	Protein phosphatase 1, regulatory (inhibitor) subunit 3C (Mm.24724; AK078506)
GCTTGTGACGA	35	22	**75** ↑	32	Transaldolase 1 (Mm.29182, NM_011528)
TCA cycle/ATP production					
CAACTGTATTT	31	16	27	**57** ↑	Aconitase 2, mitochondrial (Mm.154581, BC004645)
GCTGTCCCAGG	1	1	0	**35** ↑	Adenylate kinase 1 (Ak1) (Mm.29189, BC014802)
AACCCTAATAA	53	58	**11** ↓	48	ATP synthase F0 subunit 6 (NC_005089, Pos:8129)
TTGATGTATCT	43	40	**4** ↓	5 ↓	ATP synthase F0 subunit 8 (NC_005089, Pos:7788)
GTTCTTTCGTG	12	10	14	**48** ↑	ATP synthase, H+ transporting, mitochondrial F0 complex, subunit c (subunit 9), isoform 2 (Mm.10314, BC006813) ESTs (Mm.146141, BI651446; Mm.371910, W10656; Mm.180356, AV009312; Mm.29827, BB025380)
GCCGAGCATAA	23	22	40	**71** ↑	ATP synthase, H+ transporting, mitochondrial F0 complex, subunit f, isoform 2 (Mm.133551, NM_020582)
CGGGAGATGCT	53	34	41	**109** ↑	ATP synthase, H+ transporting, mitochondrial F1 complex, O subunit (Mm.41, NM_138597)
GCATACGGCGC	13	11	37	**51** ↑	ATP synthase, H+ transporting, mitochondrial F1F0 complex, subunit e (Mm.136093, NM_007507)
CCCTGCCTTAA	44	47	43	**366** ↑	Creatine kinase, muscle (Mm.2375, AK009950)
AGGACAAATAT	278	247	**38** ↓	143	Cytochrome b (NC_005089, Pos:14548)
GGCTAGATTTC	59	29	**2** ↓	11	Cytochrome c oxidase subunit I (NC_005089, Pos:5739)
TGGTGTAAGCA	14	14	6	**113** ↑	Cytochrome c oxidase subunit I (NC_005089, Pos:6673)
ATGAGAACAGC	3	1	14	**19** ↑	Cytochrome c oxidase subunit I (NC_005089, Pos:6728)
AAGTCATTCTA	25	10	**39** ↑	31	Cytochrome c oxidase subunit I (NC_005089, Pos:6813)
AGTGGAGGACG	34	45	39	**157** ↑	Cytochrome c oxidase subunit II (NC_005089, Pos:7497)
AGCAGTCCCCT	249	200	402	**696** ↑	Cytochrome c oxidase subunit II (NC_005089, Pos:7500)
CTGCGGCTTCA	9	7	**37** ↑	**53** ↑	Cytochrome c oxidase subunit III (NC_005089, Pos:9322)
GAGGGGCAGGA	3	3	2	**30** ↑	Cytochrome c oxidase, subunit VI a, polypeptide 2 (Mm.43824, U08439)
AATATGTGTGG	45	56	**159** ↑	128	Cytochrome c oxidase, subunit VIc (Mm.548; AK013459)
ACGCTGACTCT	1	2	1	**43** ↑	Cytochrome c oxidase, subunit VIIa 1 (Mm.12907, AK079950)
TGATATGAGCT	7	3	9	**29** ↑	Lactate dehydrogenase 2, B chain (Mm.9745; NM_008492)
TCTTTGGAACC	22	14	27	**70** ↑	Malate dehydrogenase 2, NAD (mitochondrial) (Mm.297096, NM_008617)
GGCACTGCGGC	9	10	24	**37** ↑	NADH dehydrogenase 1 alpha subcomplex 11 (Mm.279823, XM_128696)
AAGGATGTGCC	17	16	37	**63** ↑	NADH dehydrogenase 1 alpha subcomplex, 13 (Mm.21162, NM_023312)
CAGAATGTGCT	21	16	32	**60** ↑	NADH dehydrogenase 1 alpha subcomplex, 2 (Mm.29867, NM_010885)
GGAGCCATTGG	17	11	23	**52** ↑	NADH dehydrogenase 1 alpha subcomplex, 5 (Mm.275780, BC028633)
ACTCGGATGCT	5	7	9	**31** ↑	NADH dehydrogenase 1 beta subcomplex, 2 (Mm.29415, NM_026612)
CTTGCAAGTGA	38	39	48	**117** ↑	NADH dehydrogenase 1 beta subcomplex, 9 (Mm.322294, NM_023172)
CTATTTCAAAG	9	8	**35** ↑	19	EST NADH dehydrogenase 1 beta subcomplex, 1, 7 kDa (Mm.345904, CD741351)
AGGAGGACTTA	106	120	**42** ↓	143	NADH dehydrogenase subunit 2 (NC_005089, Pos:4413)
GTAGTGGAAGT	39	52	64	**312** ↑	NADH dehydrogenase subunit 3 (NC_005089, Pos:9685)
ATTATAGTACG	2	2	7	**22** ↑	NADH dehydrogenase subunit 4 (NC_005089, Pos:11195)
TGGCTATAAGT	1	1	3	**17** ↑	NADH dehydrogenase subunit 4 (NC_005089, Pos:11236)
ACTACCATCAG	83	42	**6** ↓	13	NADH dehydrogenase subunit 5 (NC_005089, Pos:12436)
ATGATGTGAAT	25	18	**1** ↓	4	NADH dehydrogenase subunit 5 (NC_005089, Pos:12853)
GGTGGTGCTTT	27	29	31	**212** ↑	Solute carrier family 25 (adenine nucleotide translocator), member 4 (Mm.16228, XM_134169)
CCTCTCAGTAC	1	0	2	**16** ↑	EST solute carrier family 25 (adenine nucleotide translocator), member 4 (Mm.16228, BY681341)
AACTGCACACA	12	8	11	**37** ↑	Succinate dehydrogenase complex, subunit B, iron sulfur (Mm.246965; AK003052)
ATTCTGTGGTG	1	1	4	**17** ↑	Succinate-CoA ligase, ADP-forming, beta subunit (Mm.38951, BC057605)

Table 2 (*Continued*)

Tag	Intact	OVX	OVX + DHT		Description (UniGene cluster, GenBank accession number)
			3 h	24 h	
TTGACAGACAC	59	38	73	**119** ↑	Ubiquinol-cytochrome c reductase (6.4 kDa) subunit (Mm.43162, *NM_025650*); EST (Mm.337888, BY694329)
CACGGGACCAC	33	25	32	**87** ↑	Ubiquinol-cytochrome c reductase hinge protein (Mm.181721, BC011388)
Others					
TCATAATAAAC	1	1	1	**36** ↑	Adenylosuccinate synthetase like 1 (Mm.3440, BC039943)
AGCAAGATGGT	8	2	**31** ↑	12	Aminolevulinic acid synthase 1 (Mm.290578, BC022110)
GAAACTCTACT	88	62	24	**12** ↓	Cysteine dioxygenase 1, cytosolic (Mm.241056, NM_033037)
CTCAGGTCTCC	5	5	4	**128** ↑	Myoglobin (Mm.201606, BC025172)

Abbreviations: OVX, ovariectomy; DHT, dihydrotestosterone; Pos., position on the mitochondrial genome. Numbers indicate the count of serial analysis of gene expression (SAGE) tags per 100 000. SAGE tag numbers in bold indicate a statistical significance ($P \leq 0.05$; OVX vs. intact, DHT vs. OVX).

transcription of mitochondrial ATP synthase F0 and F1 complexes, and the ADP/ATP transporter solute carrier family 25 member 4 (*Slc25a4*), were enhanced. This increased expression of oxidative phosphorylation-related transcripts is accompanied by an elevated expression of myoglobin as well as creatine kinase and adenylate kinase, showing a considerable up-regulation of ATP production genes.

3.3. DHT-modulated transcripts involved in Ca^{2+} release/uptake

Ca^{2+} release/uptake system represents a key intracellular regulatory mechanism which is well known to control numerous pathways. Therefore, it was interesting to find that several genes coding for Ca^{2+} channels and endoplasmic reticulum (ER)-associated Ca^{2+} binding proteins were up-regulated following DHT24 h (Table 3). Ca^{2+} ATPase, voltage-dependent L-type Ca^{2+} channel as well as histidine-rich calcium binding protein, triadin, junctin and ryanodine receptor 1 are the main transcripts whose expressions were induced. Only the expression of calreticulin was dramatically reduced by DHT. It is important to mention that all the up-regulated genes cited above are usually expressed at high levels in muscle tissues in association with sarcoplasmic reticulum (SR).

3.4. DHT-modulated transcripts involved in cell structure/motility

Cell structure associated genes, particularly those involved in motility, were found to be highly influenced by DHT treatment. In fact, 43 out of 44 transcripts were up-regulated following DHT24 h, and only gelsolin gene expression was decreased. Among the transcripts listed in Table 4, we observed many genes usually associated to muscular contraction, such as myosin light and heavy chains, actin and several actin-binding proteins, troponin I, C, and T, as well as tropomodulin, tropomyosin 1α and 2β, and myomesin. Moreover, we observed the up-regulation of transcripts in microtubule systems, such as tubulin α4, kinesin family member 1c, and ring finger protein 30. In contrast, 2 extracellular matrix (ECM)-associated transcripts were down-regulated (matrix metalloproteinase 14 and decorin).

3.5. Other differentially expressed genes following DHT treatment

In addition, DHT treatment showed modulations of a number of different genes involved in cell signalling ($n = 6$), gene–protein expression ($n = 19$) and cell defence ($n = 15$). Cyclin G1 and N-myc downstream regulated gene 2 were up-regulated, whereas protein kinase Cδ (PKCδ) and EST insulin-like growth factor binding protein 7 were down-regulated, suggesting that most cells are likely to be in a synthetic/growing phase of their cycle. Consistently, the expression of carboxypeptidase E, an important pro-hormone processing exopeptidase, as well as cold shock domain protein A, several ribosomal proteins (4 out of 6 transcripts), transcription elongation factor A and 1α2, and crystallin αB were induced, underlining a condition of enhanced protein synthesis and processing (Table 5).

Genes involved in cell defence and immunity were mainly down-regulated, including EST lysozime and lysosomal-associated membrane glycoprotein 1, EST adipsin, as well as a macrophage transcript named tartrate resistant acid phosphatase 5 (*TRAP*/*Acp5*), which is known to induce proliferation and differentiation of mouse and human adipocyte precursor cells [28].

Moreover, we found 23 partially characterized and 125 novel transcripts to be differentially modulated following DHT3 h or DHT24 h. These mainly showed an increased expression compared to OVX control, except for 13 tags which were stably down-regulated both at DHT3 h and DHT24 h (see Appendices 1 and 2). Interestingly, the SAGE tag GACCAGCAGAC was up-regulated by OVX, but DHT treatment reversed the effect.

3.6. SAGE data confirmation by Q_RT-PCR and comparison between AT and skeletal muscle most expressed genes

Since our DHT24 h SAGE data seemed to suggest the induction of a myogenic transcriptional program in adipose cells, the expression of seven myogenic transcripts significantly modulated at that time point was verified using the Q_RT-PCR method [29]. Globally, the PCR results are in good agreement with SAGE data (Fig. 1).

Moreover, we compared the 10 most expressed of the known genes presently found in intact and DHT24 h AT with the 10 most expressed ones detected by a previous SAGE analysis [14] in intact skeletal muscle. As shown in Table 6, there is an 80% overlap between intact skeletal muscle and DHT24 h genes versus a 30% between intact and DHT24 AT. Therefore, the panel of transcriptional changes induced by DHT in AT appears closer to the expected muscular expression profile.

4. Discussion

4.1. OVX, E_2 and DHT differential effects on female mice AT

The androgenicity observed in the early phases of menopause is likely to play a major role in endocrine modifications characterizing this period. We have already studied the effects of OVX and E_2 on female mice AT transcriptome [10]. We have found few effects induced by E_2, whereas OVX had mainly up-regulated ECM components, such as procollagen type 1α2, fibronectin 1 and secreted acidic cysteine rich glycoprotein (*Sparc*). Moreover, fatty acid synthase (*Fasn*) gene expression decreased compared to intact AT. The present study further confirmed those data, and additionally showed the DHT-induced down-regulation of genes highly

Table 3
Female mouse DHT-modulated transcripts involved in Ca^{2+} release/uptake.

Tag	Intact	OVX	OVX + DHT		Description (UniGene cluster, GenBank accession no.)
			3 h	24 h	
CTCACGTCGCC	0	0	3	**25** ↑	Aspartate-beta-hydroxylase (Mm.239247, AK009903)
CATCTTCAGCC	14	18	19	**399** ↑	ATPase, Ca^{2+} transporting, cardiac muscle, fast twitch 1 (Mm.35134, BC036292)
TCATCTTTAAC	15	16	**0** ↓	**0** ↓	Calreticulin (Mm.1971, AK075605)
ATACGAACCCC	1	1	1	**16** ↑	EST calcium channel, voltage-dependent, gamma subunit 1 (Mm.57093, AV084449)
TTGGAGACTCC	1	3	3	**47** ↑	Histidine-rich calcium binding protein (Mm.39968, NM_010473)
TGGGCCACCTC	4	6	6	**239** ↑	Parvalbumin (Mm.2766, AK013561)
TTTTTCCTGAT	3	3	4	**42** ↑	Ryanodine receptor 1, skeletal muscle (Mm.226037, NM_009109)
GGATTCAGAGA	1	5	1	**51** ↑	Sarcalumenin (Mm.35811, NM_175347)
GGGATTTAAAA	1	0	2	**29** ↑	Triadin (Mm.338508, XM_483889)
GGTGGGCAGGG	1	0	2	**20** ↑	Voltage-dependent L-type calcium channel alpha-1S subunit (Mm.337571, L06234)

Abbreviations: OVX, ovariectomy; DHT, dihydrotestosterone. Numbers indicate the count of serial analysis of gene expression (SAGE) tags per 100 000. SAGE tag numbers in bold indicate a statistical significance ($P \leq 0.05$; OVX vs. intact, DHT vs. OVX).

expressed in intact female retroperitoneal AT, namely EST carbonic anhydrase III, EST adipsin, ATP synthase subunit 6, EST *Fabp4*, and stearoyl-CoA desaturase 1 [10]. Interestingly, the SAGE tag GAAAATGAGAA, which has no match in the databases, was also confirmed among the 10 most expressed genes in intact AT, and its expression was reduced following DHT3 h and 24 h. This tag may be a good target for further characterization studies.

4.2. DHT effects on lipid metabolism transcripts

The present work aimed to analyze the effects of DHT on intra-abdominal AT gene expression of female mice. There is substantial evidence that intra-abdominal (retroperitoneal and visceral) fat depots possess distinct features compared to subcutaneous fat for instance [11], both at the cellular and molecular/metabolic level [30,31]. In particular, the cytokine profile as well as the contribution to insulin resistance and cardiovascular risk represent some of the differential features most extensively reported in the last years [32,33]. We have previously described the acute effects of DHT in male retroperitoneal AT [8]. In males, when the same experimental conditions were applied, lipid metabolism was mostly affected, with de novo FA synthesis, TG synthesis as well as lipolysis being up-regulated. Surprisingly, in females, few lipid metabolism-related genes were modulated. However, important transcripts such as *Scd1*, acyl-CoA synthetase long-chain family member 1 (*Acsl1*), desnutrin, EST *Lpl* and resistin were down-regulated compared to OVX control. Therefore, both lipogenesis and lipolysis appeared to be reduced. Interestingly, two transcripts coding for distinct fatty acid binding proteins (*Fabps*) showed a particular pattern of expression following DHT treatment. The different members of this lipid chaperone family (liver, intestinal, heart, adipocyte, epidermal, ileal, brain, myelin and testis) show unique patterns of expression [34]. In this study, we found that the transcription of the adipocyte member *Fabp4* was comparable in intact and OVX mice AT, and enhanced at DHT3 h. However, its level diminished to that of intact AT at DHT24 h. Conversely, at this time point, transcription of *Fabp3*, which is mostly expressed in heart and skeletal muscle, but also found in brown and white AT, was significantly increased. *Fabp3* gene is known to be regulated by androgens in muscle cells [35], but to our knowledge this is the first time that this modulation is observed in AT.

4.3. Induction of energy metabolism transcripts by DHT

In contrast with reduced lipid metabolism modulation, our data revealed a general enhancement of glucose metabolism and energy production machinery. Indeed, several mitochondrial transcripts were up-regulated, underlining a transcriptional drive to ATP production by the electron transport chain. Consistently, our DHT24 h data showed the up-regulation of an important ADP/ATP carrier, *Slc25a4*, which shuttles ADP and ATP at high specificity between mitochondria and cytosol. It is mainly expressed in heart and skeletal muscle, and plays the fundamental role to link mitochondrial energy metabolism requiring ADP with the cytosolic milieu, where ATP is consumed [36]. Moreover, myoglobin gene expression was augmented, concordant with the potentially enhanced oxidative phosphorylation and the consequent higher oxygen requirements. The cellular demand of ATP appeared to be substantial, as creatine kinase and adenylate kinase transcripts were also up-regulated. These two enzymes are usually expressed by cells rapidly consuming energy, in order to prevent the depletion of ATP stores.

4.4. Induction of calcium signalling transcripts by DHT

Intracellular Ca^{2+} signalling system has also been modulated at DHT24 h. Eleven transcripts were affected and only calreticulin, a Ca^{2+} binding chaperone which plays an important role for Ca^{2+} buffering in non-muscle cells [37] was down-regulated. Overall, the expression of several important genes for Ca^{2+} uptake/release was increased. Seven of these genes are known to code for important SR-associated molecules. In particular, ryanodine receptor 1, junctin, and triadin are part (together with calsequestrin) of a macromolecular SR Ca^{2+} regulating complex, which is a major actor for normal Ca^{2+} release and contractility in cardiac and skeletal muscle [38,39]. Moreover, three other DHT24 h up-regulated genes are important components of the SR Ca^{2+} cycling complex: histidine-rich calcium binding protein, voltage-dependent L-type calcium channel alpha-1S subunit and Ca^{2+} ATPase.

These data are consistent with the increased expression we observed for the energy production-related transcripts and with the up-regulation of numerous motility/myogenic genes, showing an expression pattern which is normally expected in muscle cells. Nevertheless, it is interesting to note that increases of intracellular Ca^{2+} concentration have been reported to inhibit the early stages of adipogenesis in mice [40,41].

4.5. Myogenic genes induction by DHT

Recently, Zhang et al. have reported a microarray analysis of DHT acute effects on male and female retroperitoneal AT [18].

Table 4
Female mouse DHT-modulated transcripts involved in cell structure/motility.

Tag	Intact	OVX	OVX + DHT		Description (UniGene cluster, GenBank accession no.)
			3 h	24 h	
AAGATCAAGAT	89	160	77	**678** ↑	Actin (Mm.360115, AK014303; Mm.292865, M26689; Mm.297, AK088691; Mm.214950, M12866; Mm.686, BY760441), EST (Mm.213025; AA710012)
ACTAGAGAGAC	1	2	0	**20** ↑	Actinin alpha 2 (Mm.37638, AY036877)
CTTCTGAATAA	6	18	11	**254** ↑	Actinin alpha 3 (Mm.5316, NM_013456)
CCAGCCAGCGT	1	3	4	**124** ↑	Ankyrin repeat domain 23 (Mm.41421, BC022973)
CCCCTTTGGAG	0	0	0	**12** ↑	EST ankyrin repeat domain 23 (Mm.41421, BB138080)
TTCAGGGCGGG	3	6	3	**33** ↑	Bridging integrator 1 (Mm.4383; NM_009668)
GCCCCTCTCTT	11	10	4	**86** ↑	Desmin (Mm.6712, BC031760)
CTCCTGGACAC	257	185	88	**40** ↓	Gelsolin (Mm.21109, AK076156)
GTGCGATGCTG	1	1	2	**17** ↑	Kinesin family member 1C (Mm.99996, BC016221)
TGCCTGTAGGC	3	3	3	**59** ↑	Myomesin 1 (Mm.4103; NM_010867)
GTGATGCTAAG	29	51	71	**1823** ↑	Myosin light chain, phosphorylatable, fast skeletal muscle (Mm.14526, NM_016754)
TGGGCAGCCTT	1	0	1	**18** ↑	EST myosin light chain, phosphorylatable, fast skeletal muscle (Mm.14526, BY453372)
AGAGAAGAGTG	9	8	5	**52** ↑	Myosin, heavy polypeptide 1, skeletal muscle (Mm.340132, AJ293626)
CGCCTGTGTGA	5	6	1	**45** ↑	Myosin, heavy polypeptide 2, skeletal muscle (Mm.34425, AJ002521)
GAGCAGACCGT	37	55	21	**751** ↑	Myosin, heavy polypeptide 4, skeletal muscle (Mm.297382, AJ278733)
CCTACAGTTGA	29	32	46	**1270** ↑	Myosin, light polypeptide 1 (Mm.1000; AK003182) EST (Mm.342003, CB588154)
GTGGTAAGCTG	1	0	1	**21** ↑	EST myosin, light polypeptide 1 (Mm.1000, AV290771)
GACCAGAACAG	1	0	2	**14** ↑	Myosin, light polypeptide 2, regulatory, cardiac, slow (Mm.1529, NM_010861)
TCTGGAGCTTC	0	1	0	**39** ↑	Myosin, light polypeptide 3 (Mm.7353, NM_010859)
AGACTACCCCA	0	2	0	**23** ↑	Myosin, light polypeptide kinase 2, skeletal muscle (Mm.250604, BC019408)
TCCTAGCAGAT	1	0	1	**12** ↑	EST myosin XVIIIb (Mm.332583, AK077135)
TGCATCATTTC	3	3	4	**87** ↑	Myozenin 1 (Mm.439911; NM_021508)
CCTCTGTGGCT	1	3	2	**24** ↑	Nebulin-related anchoring protein (Mm.6384, NM_008733)
TAAAAATTTAC	0	2	1	**28** ↑	EST nebulin (Mm.246828, CR759458)
GCTGTAGGGTG	1	1	1	**21** ↑	Obscurin, cytoskeletal calmodulin and titin-interacting RhoGEF (Mm.38029, BC044882)
ATGTGCAGACT	2	3	2	**80** ↑	Phosphodiesterase 4D interacting protein (myomegalin) (Mm.129840, AJ290946)
GAGAGTTACAG	0	1	1	**19** ↑	Ring finger protein 28 (Mm.331961, AJ278734)
GCTTTGGATGG	1	1	0	**25** ↑	Ring finger protein 30 (Mm.143796, NM_021447)
ACCTTGTAGCT	1	0	0	**12** ↑	Sarcoglycan, alpha (dystrophin-associated glycoprotein) (Mm.18709, AK075915)
TGAGTTAGTGG	2	0	1	**27** ↑	EST synaptopodin 2 (Mm.317009, AK004418)
CTTGCTGTTTG	0	0	0	**12** ↑	EST synaptopodin 2-like (Mm.35789, AK084541)
CCAGTATATGT	4	5	4	**30** ↑	Titin (Mm.46242, AK003152)
GATAGCTTGGG	2	5	3	**120** ↑	Titin (Mm.46242, BC025840)
ACCCGGAACAA	1	1	1	**25** ↑	Tropomodulin 4 (Mm.71935, BC068020)
AAAGTCATTGA	33	49	39	**534** ↑	Tropomyosin 1, alpha (Mm.121878, AK077713)
GACGCCATCAA	0	1	0	**18** ↑	EST tropomyosin 1, alpha (Mm.121878, AW229930)
CACTGACCTCC	17	13	17	**86** ↑	Tropomyosin 2, beta (Mm.646, AK003186)
TGACAGAAGAG	24	34	25	**902** ↑	Troponin C2, fast (Mm.1716, NM_009394)
GAGGGCCGGAA	22	37	38	**1049** ↑	Troponin I, skeletal, fast 2 (Mm.39469, NM_009405)
ACCTGCTGTGT	0	4	3	**29** ↑	Troponin T1, skeletal, slow (Mm.358643; AF020946) EST (Mm.361853; BG795511)
GGTGCCAACTA	21	42	12	**413** ↑	Troponin T3, skeletal, fast (Mm.389992, NM_011620)
ACTGTCCGGGC	10	5	13	**527** ↑	Troponin T3, skeletal, fast, isoform FB1e16 (Mm.350054, L48990)
CTGAGCAACAC	2	1	0	**16** ↑	Tubulin, alpha 4 (Mm.1155, M13444)
TGTGTCAACCT	2	4	**23** ↑	5	Tyrosine 3-monooxygenase/tryptophan 5-monooxygenase activation protein, eta polypeptide (Mm.332314; NM_011738) EST (Mm.354610; BB833023)
Extracellular matrix					
TGTTCATCTTG	110	**325** ↑	261	155	Collagen, type III, alpha 1 (Mm.249555; NM_009930)
AGAATGAGATC	45	48	**5** ↓	**7** ↓	Decorin (Mm.56769, X53929)
CCAACGCTTTA	17	**59** ↑	69	44	Fibronectin 1 (Mm.193099; BC004724)
GGACGCCCAAG	8	20	**2** ↓	**2** ↓	Matrix metalloproteinase 14 (membrane-inserted) (Mm.280175, NM_008608)
CAATGTGGGTT	14	**57** ↑	47	30	Periostin, osteoblast specific factor (Mm.236067; BC031449)
CGCCTGCTAGC	42	**155** ↑	93	60	Procollagen, type I, alpha 2 (Mm.277792; BC042503)
GTTCCAAAGAA	10	**52** ↑	77	58	Procollagen, type I, alpha 2 (RIKEN full-length enriched library, clone:1200014H15) (Mm.277792; AK075707)
TCTTCTATGCA	7	**40** ↑	44	50	EST procollagen, type I, alpha 2 (Mm.277792; CB575147)

Abbreviations: OVX, ovariectomy; DHT, dihydrotestosterone. Numbers indicate the count of serial analysis of gene expression (SAGE) tags per 100 000. SAGE tag numbers in bold indicate a statistical significance ($P \leq 0.05$; OVX vs. intact, DHT vs. OVX).

Table 5
Other transcripts differentially expressed following DHT treatment in female mice.

Tag	Intact	OVX	OVX + DHT		Description (UniGene cluster, GenBank accession no.)
			3 h	24 h	
Cell signaling					
TAATGGATAAG	7	5	1	**25** ↑	Cyclin G1 (Mm.2103, BC005534)
AGCCTCTGTAG	17	18	**1** ↓	5	EST insulin-like growth factor binding protein 7 (Mm.233470, BE850065)
TAAAAAGAAAG	8	8	5	**53** ↑	N-myc downstream regulated gene 2 (Ndrg2) (Mm.26722; NM_013864)
CTGGATATTTC	2	1	0	**12** ↑	EST N-myc downstream regulated gene 2 (Mm.26722, BY614809)
CTGGAGGCTCT	9	19	**1** ↓	**1** ↓	Protein kinase C, delta binding protein (Mm.3124, NM_028444)
CCCAGCGCTTG	0	0	0	**11** ↑	EST sodium channel, type IV, beta polypeptide (Mm.335112, BC050045)
Gene-protein expression and post-transcriptional processes					
ACCGTGGGCCA	0	2	0	**20** ↑	ADP-ribosyltransferase 1 (Mm.261071; AK003107) EST (Mm.261071; W41430)
ATCCTGGTAAT	3	3	2	**21** ↑	Carboxypeptidase E (Mm.31395, NM_013494)
CCCCAGGAGAG	4	3	4	**32** ↑	Chaperone, ABC1 activity of bc1 complex like (S. pombe) (Mm.38330, NM_023341)
CAAATGAAGTG	1	5	19	**29** ↑	Cold shock domain containing E1, RNA binding (Mm.277713; BC062097)
ATTTAAGAAGA	6	6	9	**34** ↑	Cold shock domain protein A (Mm.299604, AF248546)
GCTTCATCTCC	9	3	4	**25** ↑	Crystallin, alpha B (Mm.178, NM_009964)
CTCACAAGGGG	1	1	**13** ↑	6	EST ewing sarcoma breakpoint region 1 (Mm.142822, AA915168)
ATGGCCAGGGC	4	2	4	**32** ↑	EST reproductive homeobox on X chromosome, 9 (Mm.156958, BM251052)
GCTGCCCTCCG	5	5	10	**25** ↑	EST ribosomal protein L32 (Mm.104368, CA467963)
TCTGCACCTCC	3	1	3	**51** ↑	Eukaryotic translation elongation factor 1 alpha 2 (Mm.2645, NM_007906)
GATTCCGTGAG	39	54	125	**144** ↑	Ribosomal protein L37 (Mm.10474; AK012544) EST (Mm.361657; BU530511)
TAAGATGTCTG	2	1	2	**57** ↑	Ribosomal protein L3-like (Mm.46198, NM_025425)
TCTGTGCACCT	13	10	34	**40** ↑	Ribosomal protein S11 (Mm.196538; NM_013725) ESTs (Mm.338250, AV153457; Mm.4985, AV061118; Mm.316362, U93864; Mm.347690, AA269463; Mm.325693, BY398653)
GCAGAGTGCGC	35	51	**14** ↓	25	Ribosomal protein S6 (Mm.325584, AK028205; Mm.361402, BY761808)
TTCAGCTCGAG	13	22	**3** ↓	10	Ribosomal protein S7 (Mm.371579; NM_011300)
GCCAGAAGGAT	1	0	1	**15** ↑	SET and MYND domain containing 1 (Mm.234274, BC076601)
AGTTCACAGAA	1	1	4	**15** ↑	SET and MYND domain containing 2 (Mm.156895; NM_026796) EST (Mm.18810; BB190792)
ACCACTTTTGT	1	1	0	**33** ↑	Transcription elongation factor A, 3 (Mm.112, AJ223472)
Cell defence					
TGGAGATAAGC	21	19	18	**2** ↓	Acid phosphatase 5, tartrate resistant (Mm.46354, NM_007388)
AGATCTGCCCC	13	3	8	**25** ↑	ATPase, H+ transporting, V1 subunit G isoform 1 (Mm.371615, AK010131; EST Mm.29868, AA051794)
CTAGTGGTGGT	11	12	**0** ↓	**0** ↓	CD1d1 antigen (Mm.1894, BC055902)
ACCCTAGTATG	7	14	1	**0** ↓	Complement component 1, q subcomponent, alpha polypeptide (Mm.439957, AK002655)
ACATCCTGAGG	63	31	18	**5** ↓	EST adipsin (Mm.4407, AA450423)
GCGAGCACACT	5	12	**0** ↓	**0** ↓	EST lysozyme (Mm.45436, BI695557)
GAAGCCAACCC	23	21	**3** ↓	**2** ↓	EST selenoprotein P, plasma, 1 (Mm.392203, BF533736)
CAGTGCAACTC	7	**36** ↑	27	9 ↓	EST Selenoprotein P, plasma, 1 (Mm.392203; BB771510)
GATTGAGAATA	1	0	**13** ↑	2	Histocompatibility 2, D region locus 1 (Mm.33263, X00246)
TTGATCCCCAT	25	31	**0** ↓	**2** ↓	Lysosomal-associated membrane glycoprotein 1 (Mm.16716; AY069968)
TAACTGACAAT	4	6	**31** ↑	17	Metallothionein 2 (Mm.147226, NM_008630)
AATTAAAAACA	63	43	**125** ↑	46	Microsomal glutathione S-transferase 1 (Mm.14796, BC009155)
ATTGGGGGAGG	9	11	**57** ↑	25	Osteoclast inhibitory lectin (Mm.197536, AY320031)
CAGGAGGAGTT	16	20	5	**2** ↓	Protein disulfide isomerase associated 3 (Mm.263177, NM_007952)
GGTCGTGTATA	20	24	12	**4** ↓	Serine (or cysteine) proteinase inhibitor, clade G, member 1 (Mm.38888, BC002026)

Abbreviations: OVX, ovariectomy; DHT, dihydrotestosterone. Numbers indicate the count of serial analysis of gene expression (SAGE) tags per 100 000. SAGE tag numbers in bold indicate a statistical significance ($P \leq 0.05$; OVX vs. intact, DHT vs. OVX).

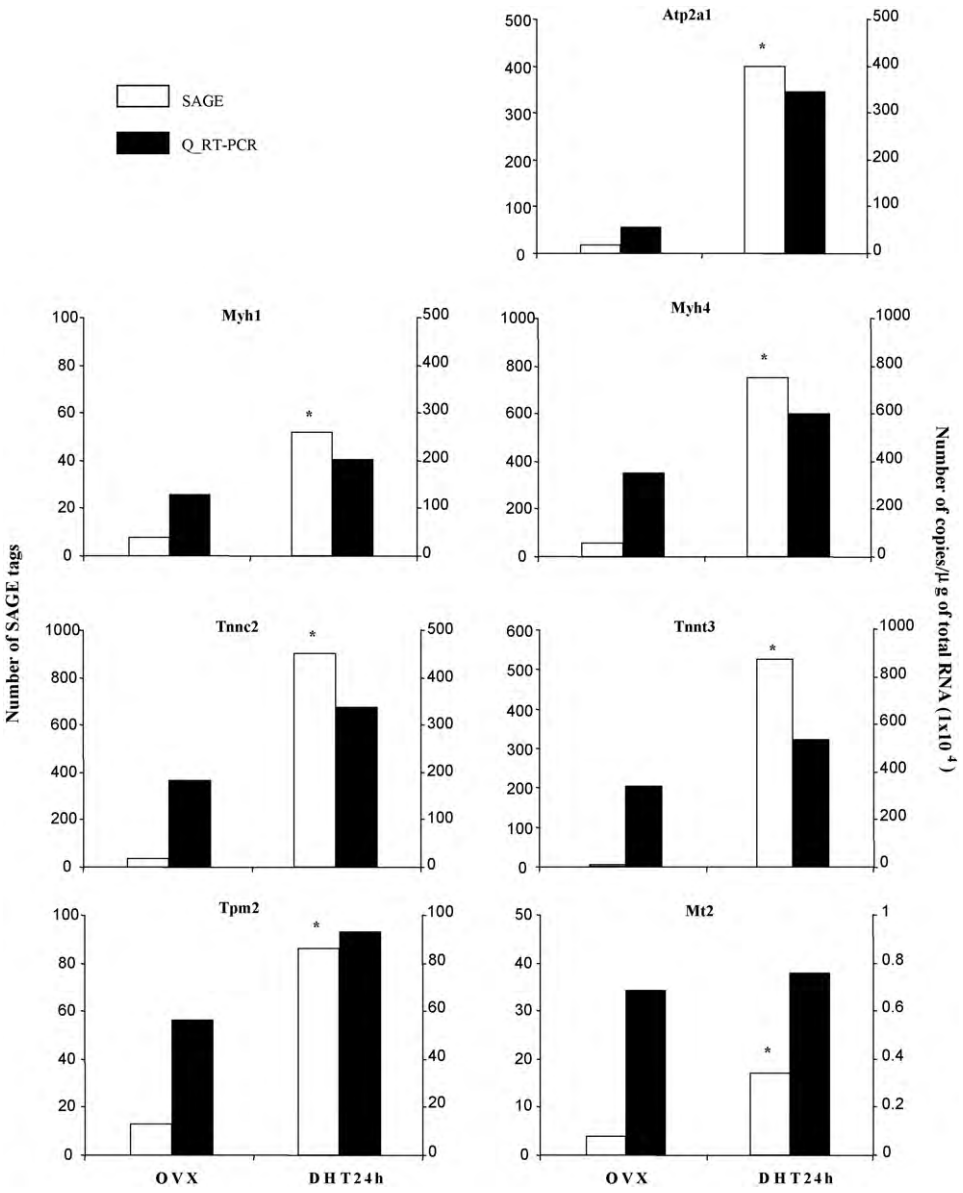

Fig. 1. Confirmation of the serial analysis of gene expression (SAGE) data by the quantitative real-time PCR (Q_RT-PCR). Asterisk represents a significant difference compared to the OVX group ($P \leq 0.05$). Abbreviations: *Atp2a1*, ATPase Ca^{2+} transporting; *Myh1*, myosin heavy polypeptide 1, skeletal muscle; *Myh4*, myosin heavy polypeptide 4, skeletal muscle; *Tnnc2*, troponin C, skeletal fast; *Tnnt3*, troponin T3, skeletal fast; *Tpm2*, tropomyosin 2, beta; *Mt2*, metallothionein 2.

SAGE and microarray are two distinct techniques with different but complementary features, whose choice depends on the specific experimental design and its final goal. They both are reliable and sensitive high-throughput transcript profiling technologies. Compared to microarray, SAGE may show less sensitivity in detecting the differential expression of low abundance mRNAs with a statistical significance, and can miss shorter transcripts which do not contain an NlaIII restriction site. However, it is a sequencing-based method that does not require prior knowledge of sequences to be analyzed, and thus offers a gene discovery potential. Moreover, the gene expression levels detected by SAGE represent the proportion of actual expression levels in the cells or tissue. The data analysis is less complex, and results are more easily reproducible and comparable among different laboratories. Indeed, studies that have compared SAGE and Affymetrix data showed that they present similar levels of sensitivity [42,43], although the SAGE method was found to be more quantitatively reproducible [44]. In their work, Zhang and his colleagues found that, in both male and female mice, DHT modulated several genes involved in the regulation of adipogenesis, with their results indicating a reduced adipogenic differentiation. They also observed that a number of genes which were significantly modulated in both sexes are myogenic in nature. Our SAGE data, obtained from the same female mice used by Zhang et al., are consistent with their conclusion and show a more extensive picture of the transcriptional myogenic program induced by DHT in female AT. They found by Affymetrix that 116 probesets (112 genes) were differentially modulated by DHT in female mice, and validated these results by Q_RT-PCR analysis for 98 transcripts. Overlapping the results of the three distinct but complementary techniques gives us a global image of the transcriptional program induced by DHT. Microarray analysis indicated a negative modulation of adipogenesis and suggested a possible myogenic response induced by DHT in AT. The information related to myogenesis is not only confirmed but further extended by SAGE study, in which more than 30% (55 out of 182) of the tags are

Table 6
The 10 most expressed genes in female mouse intact adipose tissue (AT) and AT 24 h after DHT administration (DHT24 h), compared with the 10 most expressed genes in intact skeletal muscle (SM).

SAGE tag	Gene name	Rank		
		AT		SM
		Intact	DHT24 h	Intact
AGCCAAAGGAA	Fatty acid binding protein 4	**1**	**5**	>100
AGGACAAATAT	Cytochrome b	**2**	26	>100
ATGCAGGGCCA	Fatty acid synthase	**3**	32	
CTCCTGGACAC	Gelsolin	**4**	97	>100
AGCAGTCCCCT	Cytochrome c oxidase subunit II	**5**	**7**	>100
CCTACTAACCA	Aldolase 1, A isoform	**6**	**9**	**7**
TTGTCAGGTAG	Malic enzyme 1	**7**	48	
TGTTCATCTTG	Collagen, type III, alpha 1	**8**	23	
AGGAGGACTTA	NADH dehydrogenase subunit 2	**9**	27	38
ACAAGTCTCTG	EST lipoprotein lipase	**10**	>100	
GTGATGCTAAG	Myosin light chain, phosphorylatable, fast skeletal muscle	47	**1**	**1**
CCTACAGTTGA	Myosin, light polypeptide 1	46	**2**	**2**
GAGGGCCGGAA	Troponin I, skeletal, fast 2	83	**3**	**3**
TGACAGAAGAG	Troponin C2, fast	75	**4**	**4**
GAGCAGACCGT	Myosin, heavy polypeptide 4, skeletal muscle	35	**6**	**6**
AAGATCAAGAT	Actin	24	**8**	**5**
AAAGTCATTGA	Tropomyosin 1, alpha	40	**10**	**8**
ACTGTCCGGGC	Troponin T3 skeletal fast	>100	12	**9**
GGTGCCAACTA	Troponin T3 skeletal fast	84	13	**10**

myogenic in nature or mainly expressed in muscular tissues. In addition, SAGE data showed a more global picture, in which the up-regulation of ATP production and calcium release related mRNAs, together with the reduced expression of important lipid metabolism genes concordantly suggest a myogenic-like transcriptional program. Table 6 compares the 10 most abundant known transcripts found by SAGE in intact female mouse AT and skeletal muscle [14], with the 10 most expressed known genes in female DHT24 h AT. The 80% overlap between the intact skeletal muscle and DHT24 h AT 10 most expressed genes further supports that DHT may have induced a myogenic-like transcriptional program in retroperitoneal adipocytes. It should be noted that both adipocytes and muscular cells derive from the same precursors, the mesenchymal pluripotent cells [45]. Testosterone and DHT are well known to promote the myogenic commitment of pluripotent precursor cells, and to inhibit adipogenesis through an androgen receptor-mediated pathway [45,46]. This is associated, at an early stage, with the activation of muscle-specific transcription factors (such as myo D, myogenin, and myf 5), and is followed by the expression of desmin and myosin heavy chain II (*Myh2*) in terminally differentiated cells. Our data showed no differential expression for the early markers, though we found a substantial up-regulation of at least five specific markers of differentiated muscle cells, namely Desmin, *Myh2*, *Tnnt1*, Actinin alpha 2 (*Actn2*), Actin, hence further suggesting a substantial myogenic trend in transcription.

4.6. Distinct gender effects of DHT on AT transcription: acute and chronic studies

The present results appear in contradiction with our previous acute study of DHT effects in male mice [8]. In males, in fact, lipid metabolism was globally affected, and the up-regulation of transcripts involved in cell structure reorganization likely indicated the stimulation of adipogenetic differentiation. In a following work, however, when the physiological dose of DHT was administered chronically, the effects on lipid metabolism stabilized toward an increased lipid mobilization, whereas FA and TG synthesis appeared to be reduced [9]. Globally, we concluded that the chronic androgen treatment may help to improve the metabolic profile of intra-abdominal AT. A similar chronic approach in females is needed to verify the extent of the myogenic induction engendered by androgens in intra-abdominal AT. However, it should be noted that the androgenicity characterizing the transition phase to menopause is a transient heterogeneous state, whose extent and duration are still hardly predictable, mostly because of a marked inter-individual variability in both estrogen and androgen levels [2]. In the present study, indeed, we were especially interested in understanding the initial events triggered by androgen predominance in the early phases of menopause, and substantiating the hypothesis that changed androgen levels may acutely affect gene expression in AT and possibly engender central fat accumulation. Finally, though a distinct gender regulation is apparent, the hypothesis that androgen may induce the transdifferentiation of mature adipocytes into muscle-like energy-expending cells offers another potential direction for improving the metabolic profile, and should be verified in finely designed chronic studies.

4.7. Plasticity potential of AT

Several studies have already been published which show the transdifferentiation potential of AT-derived cells, and that they can be committed into myogenic, chondrogenic, osteogenic cells, as well as other non-mesenchymal lineages [47]. In particular, the myogenic potential has already been demonstrated for mouse pluripotent [46], preadipose [48] and mature fat cells [49], and has been recently employed for successful muscle regeneration in human and mouse models of Duchenne muscular dystrophy [50–52]. These results have opened new scenarios in which it would be possible, for instance, to use AT as a source of stem cells therapies for muscular diseases. We do believe that the extensive plasticity shown by AT in this and other works [47,49] is a topic of critical interest which should be better and sooner addressed as another promising key target to prevent and treat intra-abdominal fat accumulation and its deleterious consequences.

In conclusion, we have analyzed the acute effects of DHT on the intra-abdominal AT gene expression in OVX mice. We have observed the modulation of few genes involved in lipid metabolism, whereas several transcripts related to skeletal muscle and muscular contraction were up-regulated. Concordantly, the expression of genes involved in glucose metabolism, ATP production as well as Ca^{2+} uptake/release cycle increased. Remarkably, the first 4 most expressed genes in DHT24 h AT exactly correspond to the 4 most

expressed in female intact skeletal muscle (Table 6), as found by SAGE method. We concluded that, 24 h after a single dose of DHT, the retroperitoneal AT gene expression may have changed toward a myogenic-like transcriptional program. These results represent an important first step toward a better understanding of gender influence on intra-abdominal AT physiology. Further studies which would verify the effects of chronic androgen prevalence will help the comprehensive understanding of menopause endocrinology and verify their potential as therapeutic targets for preventing and/or treating the intra-abdominal obesity associated with this condition.

Author's contributions and declarations of interest

The present article has been approved by all listed authors and there is no conflict of interest that would prejudice its impartiality. MRDG analyzed and interpreted the SAGE data, and drafted the manuscript. MY and JstA conceived the study, designed it and critically revised the manuscript. JstA gave the final approval of the version to be published.

Acknowledgements

We would like to thank Dr. Ping Ye for the SAGE analysis; Dr. André Tchernof and Dr. Yonghua Zhang for giving us the permission to use some of the PCR data they had previously collected for their microarray study; all the research assistants and investigators involved in the ATLAS project. This work was supported by the Genome Québec and Genome Canada. J.S.-A. is supported by the Fonds de la recherché en santé du Québec (FRSQ).

Appendix A. Supplementary data

Supplementary data associated with this article can be found, in the online version, at doi:10.1016/j.jsbmb.2010.02.023.

References

[1] Y. Liu, J. Ding, T.L. Bush, J.C. Longenecker, F.J. Nieto, S.H. Golden, M. Szklo, Relative androgen excess and increased cardiovascular risk after menopause: a hypothesized relation, Am. J. Epidemiol. 154 (2001) 489–512.
[2] H.G. Burger, G.E. Hale, D.M. Robertson, L. Dennerstein, A review of hormonal changes during the menopausal transition: focus on findings from the Melbourne Women's Midlife Health Project, Hum. Reprod. Update 13 (2007) 559–565.
[3] M.J. Toth, A. Tchernof, C.K. Sites, E.T. Poehlman, Effect of menopausal status on body composition and abdominal fat distribution, Int. J. Obesity 24 (2000) 226–231.
[4] I. Janssen, L.H. Powell, S. Crawford, B. Lasley, K. Sutton-Tyrrell, Menopause and the metabolic syndrome, Arch. Intern. Med. 168 (2008) 1568–1575.
[5] C.C. Lee, J.Z. Kasa-Vubu, M.A. Supiano, Androgenicity and obesity are independently associated with insulin sensitivity in postmenopausal women, Metabolism 53 (2004) 507–512.
[6] M.A. Maturana, V. Breda, F. Lhullier, P.M. Spritzer, Relationship between endogenous testosterone and cardiovascular risk in early postmenopausal women, Metabolism 57 (2008) 961–965.
[7] Heart Disease and Stroke Statistics-2003 update, American Heart Association, Dallas, 2002.
[8] C. Bolduc, M. Larose, M. Yoshioka, P. Ye, P. Belleau, C. Labrie, J. Morissette, V. Raymond, F. Labrie, J. St-Amand, Effects of dihydrotestosterone on adipose tissue measured by serial analysis of gene expression, J. Mol. Endocrinol. 33 (2004) 429–444.
[9] C. Bolduc, M. Yoshioka, J. St-Amand, Transcriptomic characterization of the long-term dihydrotestosterone effects in adipose tissue, Obesity 15 (2007) 1107–1132.
[10] P. Ye, M. Yoshioka, L. Gan, J. St-Amand, Regulation of global gene expression by ovariectomy and estrogen in female adipose tissue, Obesity 13 (2005) 1024–1030.
[11] S. Klein, The case of visceral fat: argument for the defense, J. Clin. Invest. 113 (2004) 1530–1532.
[12] S.Z. Haslam, Ovariectomized mouse model for human menopause, Board of Trustees operating Michigan State University, US Patent no. 6583334 (2000).
[13] M. Yoshioka, A. Boivin, P. Ye, F. Labrie, J. St-Amand, Effects of dihydrotestosterone on skeletal muscle transcriptome in mice measured by serial analysis of gene expression, J. Mol. Endocrinol. 36 (2006) 247–259.
[14] M. Yoshioka, A. Boivin, C. Bolduc, J. St-Amand, Gender difference of androgen actions on skeletal muscle transcriptome, J. Mol. Endocrinol. 39 (2007) 119–133.
[15] L. Azzi, M. El-Alfy, C. Martel, F. Labrie, Gender differences in mouse skin morphology and specific effects of sex steroids and dehydroepiandrosterone, J. Invest. Dermatol. 124 (2005) 22–27.
[16] M. Ivanga, Y. Labrie, E. Calvo, P. Belleau, C. Martel, G. Pelletier, J. Morissette, F. Labrie, F. Durocher, Fine temporal analysis of DHT transcriptional modulation of the ATM/Gadd45g signaling pathways in the mouse uterus, Mol. Reprod. Dev. 76 (2009) 278–288.
[17] C. Ma, M. Yoshioka, A. Boivin, L. Gan, Y. Takase, F. Labrie, J. St-Amand, Atlas of dihydrotestosterone actions on the transcriptome of prostate in vivo, Prostate 69 (2009) 293–316.
[18] Y. Zhang, E. Calvo, C. Martel, V. Luu-The, F. Labrie, A. Tchernof, Response of the adipose tissue transcriptome to dihydrotestosterone in mice, Physiol. Genomics 35 (2008) 254–261.
[19] M.K. Angele, A. Ayala, B.A. Monfils, W.G. Cioffi, K.I. Bland, I.H. Chaudry, Testosterone: the culprit for producing splenocyte immune depression after trauma hemorrhage, Am. J. Physiol. 274 (1998) C1530–1536.
[20] V. Kahlke, M.K. Angele, A. Ayala, M.G. Schwacha, W.G. Cioffi, K.I. Bland, I.H. Chaudry, Immune dysfunction following trauma-haemorrhage: influence of gender and age, Cytokine 12 (2000) 69–77.
[21] V.E. Velculescu, L. Zhang, B. Vogelstein, K.W. Kinzle, Serial analysis of gene expression, Science 270 (1995) 484–487.
[22] J. St-Amand, K. Okamura, K. Matsumoto, S. Shimizu, Y. Sogawa, Characterization of control and immobilized skeletal muscle: an overview from genetic engineering, FASEB J. 15 (2001) 684–692.
[23] S. Dinel, C. Bolduc, P. Belleau, A. Boivin, M. Yoshioka, E. Calvo, B. Piedboeuf, E.E. Snyder, F. labrie, J. St-Amand, Reproducibility, bioinformatics analysis and power of the SAGE method to evaluate changes in transcriptome, Nucleic Acids Res. 33 (2005) e26.
[24] M.D. Adams, A.R. Kerlavage, R.D. Fleischmann, R.A. Fuldner, C.J. Bult, N.H. Lee, E.F. Kirkness, K.J. Weinstock, J.D. Gocayne, O. White, Initial assessment of human gene diversity and expression patterns based upon 83 million nucleotides of cDNA sequence, Nature 377 (1995) 3–174.
[25] V. Luu-The, N. Paquet, E. Calvo, J. Cumps, Improved real-time RT-PCR method for high-throughput measurements using second derivative calculation and double correction, Biotechniques 38 (2005) 287–293.
[26] A.E. Lash, C.M. Tolstoshev, L. Wagner, G.D. Schuler, R.L. Strausberg, G.J. Riggins, S.F. Altschul, SAGEmap: a public gene expression resource, Genome Res. 10 (2000) 1051–1060.
[27] S. Welle, K. Bhatt, C.A. Thornton, Inventory of high-abundance mRNAs in skeletal muscle of normal men, Genome Res. 9 (1999) 506–513.
[28] P. Lang, V. van Harmelen, M. Rydén, M. Kaaman, P. Parini, C. Carneheim, A.I. Cassady, D.A. Hume, G. Andersson, P. Arner, Monomeric tartrate resistant acid phosphatase induces insulin sensitive obesity, PLoS ONE 3 (2008) e1713.
[29] A. Menssen, H. Hermeking, Characterization of the c-MYC-regulated transcriptome by SAGE: identification and analysis of c-MYC target genes, Proc. Natl. Acad. Sci. U S A 99 (2002) 6274–6279.
[30] C. Poussin, D. Hall, K. Minehira, A.M. Galzin, D. Tarussio, B. Thorens, Different transcriptional control of metabolism and extracellular matrix in visceral and subcutaneous fat of obese and rimonabant treated mice, PLoS One 3 (2008) e3385.
[31] S. Gesta, M. Blüher, Y. Yamamoto, A.W. Norris, J. Berndt, S. Kralisch, J. Boucher, C. Lewis, C.R. Kahn, Evidence for a role of developmental genes in the origin of obesity and body fat distribution, Proc. Natl. Acad. Sci. U S A 103 (2008) 6676–6681.
[32] L. Laviola, S. Perrini, A. Cignarelli, F. Giorgino, Insulin signalling in human adipose tissue, Arch. Physiol. Biochem. 112 (2006) 82–88.
[33] Y. Matsuzawa, The role of fat topology in the risk of disease, Int. J. Obes. (Lond.) 32 (2008) S83–92.
[34] M. Furuhashi, G.S. Hotamisligil, Fatty acid binding proteins: role in metabolic diseases and potential as drug targets, Nature Rev. 7 (2008) 489–503.
[35] E. van Breda, H.A. Keizer, M.M. Vork, D.A. Surtel, Y.F. de Yong, G.J. van der Vusse, J.F. Glatz, Modulation of fatty-acid-binding protein content of rat heart and skeletal muscle by endurance training and testosterone treatment, Pflügers Archiv: Eur. J. Physiol. 421 (1992) 274–279.
[36] F. Palmieri, The mitochondrial transporter family (SLC25): physiological and pathological implications, Pflügers Archiv: Eur. J. Physiol. 447 (2004) 689–709.
[37] P. Gelebart, M. Opas, M. Michalak, Calreticulin, a Ca^{2+}-binding chaperone of the endoplasmic reticulum, Int. J. Biochem. Cell B 37 (2005) 260–266.
[38] L. Zhang, J. Kelley, G. Schmeisser, Y.M. Kobayashi, L.R. Jones, Complex formation between junctin, triadin, calsequestrin, and the ryanodine receptor, J. Biol. Chem. 272 (1997) 23389–23397.
[39] Q. Yuan, Q.-C. Fan, M. Dong, et al., Sarcoplasmic reticulum calcium overloading in junctin deficiency enhances cardiac contractility but increases ventricular automaticity, Circulation 115 (2007) 300–309.
[40] H. Shi, Y.-D. Halvorsen, P.N. Ellis, W.O. Wilkinson, M.B. Zemel, Role of intracellular calcium in human adipocyte differentiation, Physiol. Genomics 3 (2000) 75–82.
[41] J.W. Neal, N.A. Clipstone, Calcineurin mediates the calcium-dependent inhibition of adipocyte differentiation in 3T3-L1 cells, J. Biol. Chem. 277 (2002) 49776–49781.

[42] H.-L. Kim, Comparison of oligonucleotide-microarray and serial analysis of gene expression (SAGE) in transcript profiling analysis of megakaryocytes derived from CD34+ cells, Exp. Mol. Med. 35 (2003) 460–466.
[43] S.J. Evans, N.A. Datson, M. Kabbaj, R.C. Thompson, E. Vreugdenhil, E.R. De Kloet, S.J. Watson, H. Akil, Evaluation of affymetrix gene chip sensitivity in rat hippocampal tissue using SAGE analysis. Serial analysis of gene expression, Eur. J. Neurosci. 16 (2002) 409–413.
[44] M. Ishii, S. Hashimoto, S. Tsutsumi, Y. Wada, K. Matsushima, T. Kodama, H. Aburatami, Direct comparison of GeneChip and SAGE on the quantitative accuracy in transcript profiling analysis, Genomics 68 (2000) 136–143.
[45] L.L. Herbst, S. Bhasin, Testosterone action on skeletal muscle, Curr. Opin. Clin. Nutr. 7 (2004) 271–277.
[46] R. Singh, J.N. Artaza, W.E. Taylor, N.F. Gonzales-Cadavid, S. Bhasin, Androgens stimulate myogenic differentiation and inhibit adipogenesis in C3H 10T1/2 pluripotent cells through an androgen receptor-mediated pathway, Endocrinology 144 (2003) 5081–5088.
[47] G. Di Rocco, M.G. Iachininoto, A. Tritarelli, S. Straino, A. Zacheo, A. Germani, F. Crea, M.C. Capogrossi, Myogenic potential of adipose-tissue-derived cells, J. Cell Sci. 119 (2006) 2945–2952.
[48] A. Abderrahim-Ferkoune, O. Bezy, S. Astri-Roques, C. Elabd, G. Ailhaud, E.-Z. Amri, Transdifferentiation of preadipose cells into smooth muscle-like cells: role of aortic carboxypeptidase-like protein, Exp. Cell Res. 293 (2004) 219–228.
[49] Y.C. Kocaefe, D. Israeli, M. Ozguc, O. Danos, L. Garcia, Myogenic program induction in mature fat tissue (with MyoD expression), Exp. Cell Res. 308 (2005) 300–308.
[50] A.-M. Rodriguez, D. Pisani, C.A. Dechesne, C. Turc-Carel, J.-Y. Kurzenne, B. Wdziekonski, A. Villageois, C. Bagnis, B. Breittmayer, H. Groux, G. Ailhaud, C. Dani, Transplantation of a multipotent cell population from human adipose tissue induces dystrophin expression in the immunocompetent mdx mouse, J. Exp. Med. 201 (2005) 1397–1405.
[51] Y. Liu, X. Yan, Z. Sun, et al., Flk-1+ adipose-derived mesenchymal stem cells differentiate into skeletal muscle satellite cells and ameliorate muscular dystrophy in mdx mice, Stem Cells Dev. 16 (2007) 695–706.
[52] N.M. Vieira, V. Brandalise, E. Zucconi, T. Jazedje, M. Secco, V.A. Nunes, B.E. Strauss, M. Vainzof, M. Zatz, Human multipotent adipose-derived stem cells restore dystrophin expression of Duchenne skeletal-muscle cells in vitro, Biol. Cell 100 (2008) 231–241.